Paleostress magnitudes associated with development of mountain belts: Insights from tectonic analyses of calcite twins in the Taiwan Foothills

Olivier Lacombe

TECTONICS, VOL. 20, NO. 6, PAGES 834-849, DECEMBER 2001

Paleostress magnitudes associated with development of mountain belts: Insights from tectonic analyses of calcite twins in the Taiwan Foothills

Olivier Lacombe

Laboratoire de Tectonique, Université Pierre et Marie Curie, Paris, France

Abstract. Determinations of stress magnitudes based on inversion of calcite twin data from fault-related folds in the Taiwan Foothills show a decrease of differential stresses during synfolding erosion and exhumation, suggesting that paleodepth of burial largely controlled the levels of differential stresses sustained by rocks. Regional frictional conditions linked to shallow and/or deep décollement tectonics probably also influenced stress magnitudes. Combination of the twin inversion technique with fracture analysis and rock mechanics data provides first-order estimates of principal stress values related to the major Pleistocene shortening event in Taiwan. These stress estimates are compared to previous stress estimates in fold-thrust belts and to available data on differential stress magnitudes in foreland and hinterland domains of orogens. At the scale of an entire orogenic system the most striking point is a decrease of differential stresses from the hinterland toward the foreland. This decrease not only reflects tectonic stress attenuation away from the plate boundary but also suggests a major control by the depth of deformation. Differential stresses estimated from natural deformation consequently provide an independent support to the depth-dependent strength and the frictional behavior of the upper continental crust deduced from laboratory experiments and stress measurements in deep boreholes.

1. Introduction and Scope of the Study

The study of the relationship between stress magnitudes and development of geological structures is inherently difficult. Determination of stress magnitudes associated with the tectonic history of rock masses relies upon establishing a close relationship between the state of stress and the development of a conspicuous element in the rock itself and calibrating it experimentally. Among the paleopiezometers commonly used to infer paleostresses are dislocation density in calcite [e.g., *Pfiffner*, 1982], dynamic recrystallisation of calcite and quartz [e.g., *Twiss*, 1977; *Weathers et al.*, 1979; *Kohlstedt and Weathers*, 1980], and mechanical twinning in calcite [e.g., *Jamison and Spang*, 1976]. The poor knowledge we have on the paleostress levels sustained by natural rocks is partially linked to the fact that the paleopiezometric techniques do not share the same limitations, each of them having particular conditions of application; this leads to multiple sources of methodological uncertainties which are superimposed to variability of natural phenomena.

Paper number 2001TC900019.
0278-7407/01/2001TC900019$12.00

Paleostress reconstructions have been carried out in both inner and outer domains of orogenic systems. In the inner part of orogens, fault zones formed at deep crustal levels and now exposed at the surface gave rise to numerous studies (e.g., Moine thrust [*Twiss*, 1977]; Glarus thrust [*Pfiffner*, 1982]; McConnel thrust [*Jamison and Spang*, 1976]; shear zone, Colorado [*Kohlsted and Weathers*, 1980]; shear zone, Wyoming [*Weathers et al.*, 1979]; thrusts in the Cantabrian zone, Spain [*Rowe and Rutter*, 1990]; Pioneer Landing fault zone, Appalachians [*Newman*, 1994]). Natural fault zones typically show concentrated and complex deformation, and many of the assumptions necessary for the methods for determining paleostresses are not met. Some problems which arise, for instance, in paleostress estimates based on twinning in carbonates close to fault zones [*Rowe and Rutter*, 1990; *Newman*, 1994] are due to the high finite strain of the rocks (which display grain-size reduction, rotational deformation at the grain scale or dynamic or fluid-enhanced recrystallization) and the record of local effects such as stress concentrations. Both may lead to overestimated stresses which are not representative of the far-field stress of interest.

The foreland domains of orogens, which show rocks weakly deformed at shallow crustal levels, have also been investigated in terms of both stress (or strain) orientations and stress magnitudes (Appenine foreland [*Alvarez et al.*, 1976]; Morocco [*Petit*, 1976]; Appalachian plateau [*Engelder*, 1982; *Engelder and Geiser*, 1984; *Jackson et al.*, 1989]; Sevier and Appalachian forelands [*Craddock and Van der Pluijm*, 1989; *Craddock et al.*, 1993; *Van der Pluijm et al.*, 1997]; Northern Pyrenean foreland [*Lacombe et al.*, 1994, 1996; *Rocher et al.*, 2000]; Southern Pyrenean foreland [*Gonzales-Casado and Garcia-Cuevas*, 1999]). These studies have led to regionally significant estimates of tectonic stresses within the foreland and provided new insights into the way tectonic stresses decrease away from the collision zone.

Foreland fold-thrust belts have been extensively described in terms of stress (or strain) orientations (subalpine chain [*Ferrill and Groshong*, 1993a]; Jura mountains [*Tschanz*, 1990]; Taiwan [*Lacombe et al.*, 1993, 1999; *Rocher et al.*, 1996; *Hung and Kuo*, 1999]; Hudson valley fold-thrust belt [*Harris and Van der Pluijm*, 1998]), but they have, surprisingly, received less attention in terms of stress magnitudes. Only few efforts have been to date devoted to characterize stress magnitudes associated with fold-thrust development, from the local to the regional scale (e.g., Southern Pyrenees [*Holl and Anastasio*, 1995]; Taiwan [*Lacombe et al.*, 1996]; subalpine chain [*Ferrill*, 1998]).

The aim of this paper is to bring new information about the stress levels associated with development of fault-related folds on the basis of the analysis of frontal structures of the recent and still active Taiwan fold-thrust belt, and to compare these new results to available information on the evolution of stress magnitudes with depth in compressional settings at the scale of the orogen. To this purpose, paleostress magnitudes were determined on the basis of the results of inversion of calcite twin data.

2. Method for Quantifying Paleostress Magnitudes Using Calcite Twin Data

The complete stress tensor is defined by six independent variables. Three variables describe the orientations of the three principal stresses σ_1, σ_2 and σ_3; the three remaining values describe their magnitudes. I summarize hereinafter how these six parameters can be estimated by combining inversion of calcite twin data with rock mechanics data.

2.1. Quantifying the Reduced Stress Tensor

Several methods of strain and stress analysis have been developed on the basis of calcite twin data [*Turner*, 1953; *Groshong*, 1972, 1974; *Jamison and Spang*, 1976; *Laurent et al.*, 1981, 1990; *Groshong et al.*, 1984; *Etchecopar*, 1984]. These methods are based on the widespread occurrence of *e*-twinning in calcite aggregates deformed at low pressure and temperature. *E*-twinning occurs with a change of form of part of the host crystal by an approximation to simple shear in a particular sense and direction along specific crystallographically defined *e* planes {01-12}, in such a way that the resulting twinned portion of the crystal bears a mirrored crystallographic orientation to the untwinned portion across the twin plane.

All methods of strain/stress analysis based on calcite twins share the fundamental assumption that the measured twins formed in a homogeneous stress field and were not passively rotated after formation. These methods are best applied to very small strains that can be approximated by coaxial conditions; in this case, the distinction between stress and strain is somewhat academic, and orientation of small twinning strain can be correlated with paleostress orientation [*Burkhard*, 1993].

The most commonly used technique in strain determination is that of *Groshong* [1972, 1974]. It is able to determine a strain tensor from a twin data set and to detect twins of incompatible orientations. The latter should not have formed in the determined strain field and may result from large noncoaxial deformation or superimposed strain events. These inconsistent data are either (usually) discarded as being noise, or used to run a new analysis. However, *Groshong*'s technique only efficiently separates perpendicularly superimposed strain or, in practice, superimposed strain directions lying at more than 45° [*Teufel*, 1980]. So in many cases, superimposed twinning events cannot be detected.

This paper relies on determinations of paleostress orientations and magnitudes by computerized inversion of calcite twin data [*Laurent*, 1984; *Etchecopar*, 1984]. This technique is less time-consuming than *Groshong*'s [1972, 1974] technique and provides stress tensors that can be easily compared to stress tensors deduced from fault slip analysis. Additionally, it has proven to be suitable for identifying geologically significant superimposed stress regimes in polyphase tectonics settings [e.g., *Lacombe et al.*, 1990, 1994; *Lacombe and Laurent*, 1996, and references therein]. Polyphase tectonism identified from inversion of calcite twin data is in most cases independently confirmed by fault slip analysis (e.g., Taiwan [*Lacombe et al.*, 1993, 1999; *Rocher et al.*, 1996]), whereas it can only be suspected from highly inhomogeneous strain in the same area using *Groshong*'s technique [*Hung and Kuo*, 1999]. Finally, the technique detects twinning events predating or postdating folding (i.e., strata tilting), based on consideration between principal stress axes and bedding attitude [e.g., *Lacombe et al.*, 1996].

The method assumes homogeneous state of stress at the grain scale and constant critical resolved shear stress (CRSS) for twinning τ_a (see discussion in section 2.2.1). The inversion process used herein to analyze calcite twin data is very similar to those used for fault slip data [e.g., *Etchecopar et al.*, 1981; *Angelier*, 1984], since twin gliding along the twinning direction within the twin plane is geometrically comparable to slip along a slickenside lineation within a fault plane. But the inversion process additionally takes into account both the twin planes oriented so that the resolved shear stress τ_s (the component of the shear stress along the twinning direction) was greater than τ_a (i.e., effectively twinned planes), and the twin planes oriented so that τ_s was lower than τ_a (i.e., untwinned planes). The inverse problem thus consists of finding the stress tensor that best fits the distribution of measured twinned and untwinned planes. This tensor must theoretically meet the major requirement that all the twinned planes consistent with it should sustain a resolved shear stress τ_s larger than that exerted on all the untwinned planes.

As in fault tectonics, the inversion of slip (gliding) data along twin planes leads only to four parameters of the complete stress tensor T. These four parameters, which define the reduced stress tensor T', are the orientations of the three principal stress axes and the stress ellipsoid shape ratio Φ [$\Phi = (\sigma_2-\sigma_3)/(\sigma_1-\sigma_3)$]. T' is such that the complete stress tensor T is a function of T' : $T = kT' + l\mathbf{I}$, where k and l are scalars ($k = (\sigma_1-\sigma_3) > 0$; $l = \sigma_3$) and $\mathbf{I}$ the unit matrix. The stress tensor solution is consequently searched as a reduced stress tensor T' and, in addition, the maximum differential stress $(\sigma_1-\sigma_3)$ is scaled to 1 [*Etchecopar*, 1984]. For this normalized tensor the resolved shear stress τ_s acting along any twin plane therefore varies between -0.5 and 0.5.

The first step of the inversion consists of obtaining a solution by applying a number of random tensors. For each tensor the stress components are calculated for all the twinned and the untwinned planes. However, because the resolved shear stress τ_s exerted on some untwinned planes may in practice be greater than that exerted along some twinned planes compatible with the tensor, the second step of the process consists of minimizing the function, f, ideally equal to 0, defined as

$$f = \sum_{j=1}^{N} (\tau_{sj}-\tau_{a'}),$$

where $\tau_{a'}$ is the smallest resolved shear stress applied on the twinned planes compatible with the tensor, and τ_{sj} are the resolved shear stresses applied on the N untwinned planes j such that $\tau_{sj} > \tau_{a'}$ (for more details, see *Etchecopar* [1984]). The $\tau_{a'}$ value is deduced from the inversion and corresponds to the CRSS for the normalized tensor used for calculation. The optimization process leads to the reduced stress tensor solution that includes the largest number of twinned planes and simultaneously corresponds to the smallest value of f. The orientations of the three principal stresses σ_1, σ_2, and σ_3 are calculated, as well as the value of the Φ ratio that indicates the magnitude of σ_2 relative to σ_1 and σ_3.

If many twins are found to be not consistent with the stress tensor solution (i.e., for many twinned planes, the calculated resolved shear stresses are lower than $\tau_{a'}$), the twinned planes consistent with the tensor are withdrawn, and the inversion process is repeated with the residual twinned planes and the whole set of untwinned planes; this new trial aims at identifying an additional stress tensor that may account for a significant part of the remaining (unexplained) twin data. Where polyphase tectonism has occurred, this process may allow separation of superimposed stress tensors, each of them accounting for subsets

of data. If uncorrelated, the residuals should be discarded as being noise. It is beyond the scope of this paper to discuss the procedure of separation of superimposed stress tensors and the confidence limit associated with their identification [e.g., *Lacombe et al.*, 1994; *Rocher et al.*, 1996; *Rocher*, 1999, and references therein].

2.2. Quantifying the Deviatoric Stress Tensor

Knowing the reduced stress tensor T', quantifying the deviatoric stress tensor T_D defined as

$$T_D = T - [(\sigma_1 + \sigma_2 + \sigma_3)/3]\mathbf{I}$$

requires the determination of a fifth parameter of the complete stress tensor: the scalar k ($=\sigma_1-\sigma_3$) defined in section 2.1. This determination relies on the existence of a constant CRSS for twinning τ_a and on the accurate estimate of τ_a, that corresponds to the normalized value of the CRSS for the reduced stress tensor used for calculation.

2.2.1. Assumption of a constant Critical Resolved Shear Stress for twinning. Differential stress estimates using the twin inversion technique are based on a constant CRSS τ_a for twinning. This assumption is also shared by the technique of *Jamison and Spang* [1976], which is widely used in paleostress reconstructions (with a constant CRSS of 10 MPa [e.g., *Craddock et al.*, 1993, 2000; *Gonzales-Casado and Garcia-Cuevas*, 1999]) although it does not take into account the grain-size dependence of twinning occurrence. This CRSS corresponds to the resolved shear stress acting along the twin plane and parallel to the imposed direction of twinning that must be reached to induce movement of many dislocations so that macroscopic plastic deformation occurs. Taking into account the importance of stress concentrations in nucleating twins [*Spiers*, 1982; *Wenk et al.*, 1986; *Rowe and Rutter*, 1990] linked to inhomogeneities at the grain scale, and the grain-size dependence of twinning, the assumption of a constant CRSS is considered unjustified by some [*Burkhard*, 1993; *Newman*, 1994; *De Bresser and Spiers*, 1997]. However, the sources of stress concentrations at the grain scale are numerous in natural crystals (dislocations, fractures, indenters, preexisting twins), so that the CRSS for twinning is likely to reflect the stress needed to propagate twins rather than to create them [Tullis, 1980], which reconciles the assumption of a constant CRSS for a given grain size.

Determination of deviatoric stress tensors based on inversion of calcite twin data from experimentally deformed monophase samples [*Lacombe and Laurent*, 1996; *Laurent et al.*, 2000] has not only established the reliability of the twin inversion technique, but emphasized that the CRSS is sensitive to strain hardening (Figure 1). However, the results also suggest that the CRSS for twinning can be considered constant for samples displaying a nearly homogeneous grain size. For samples displaying a mean grain size of ~200-300 μm and deformed between 0° and 100°C at 2-2.5% strain, it equals 10 MPa; for the same samples deformed at nearly 1-1.5% strain, the CRSS rather equals 5 MPa (Figure 1).

2.2.2. Determination of differential stress magnitudes. Under the assumption of a constant CRSS for twinning τ_a, the

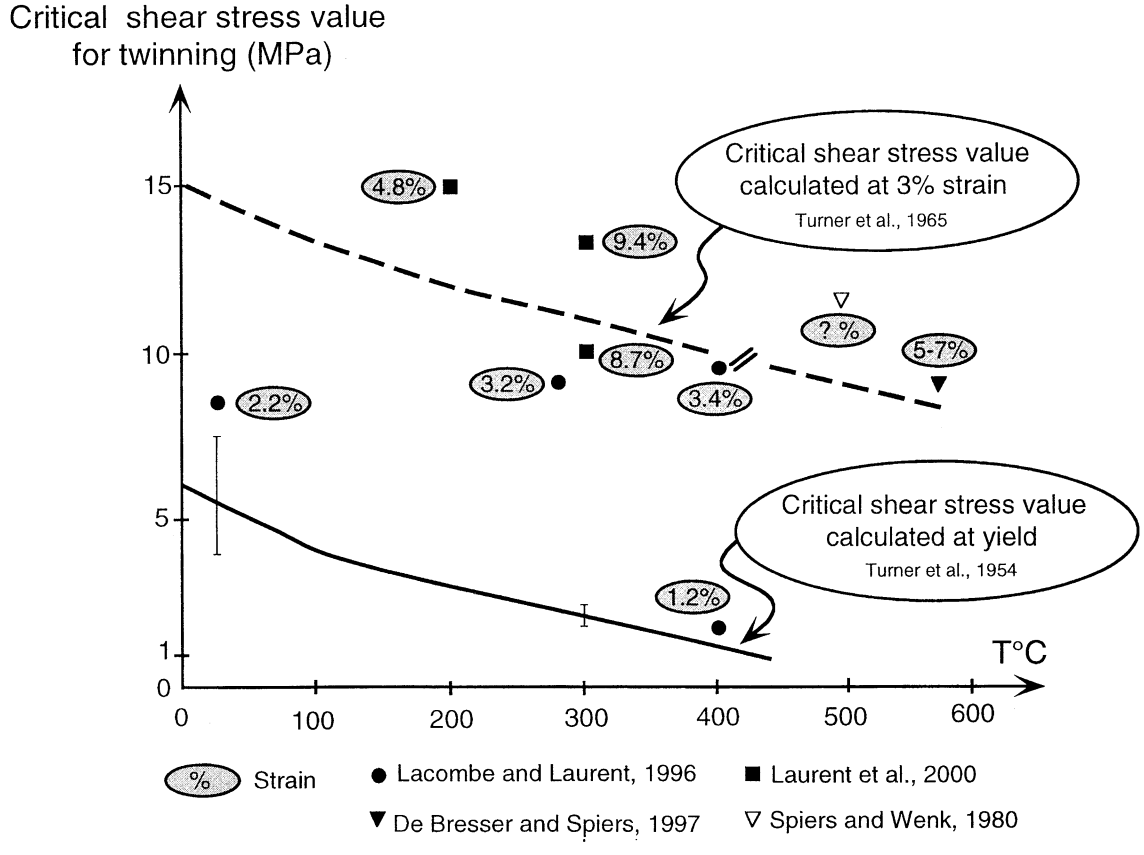

Figure 1. Critical shear stress values for calcite twinning as a function of temperature and strain inferred from laboratory experiments. A CRSS of 10 (± 5) MPa is acceptable for low strained samples (1-4%) deformed at low temperature (<150°-200°C) displaying a mean grain size of ~ 200-300 μm. Modified and completed after *Laurent et al.* [2000].

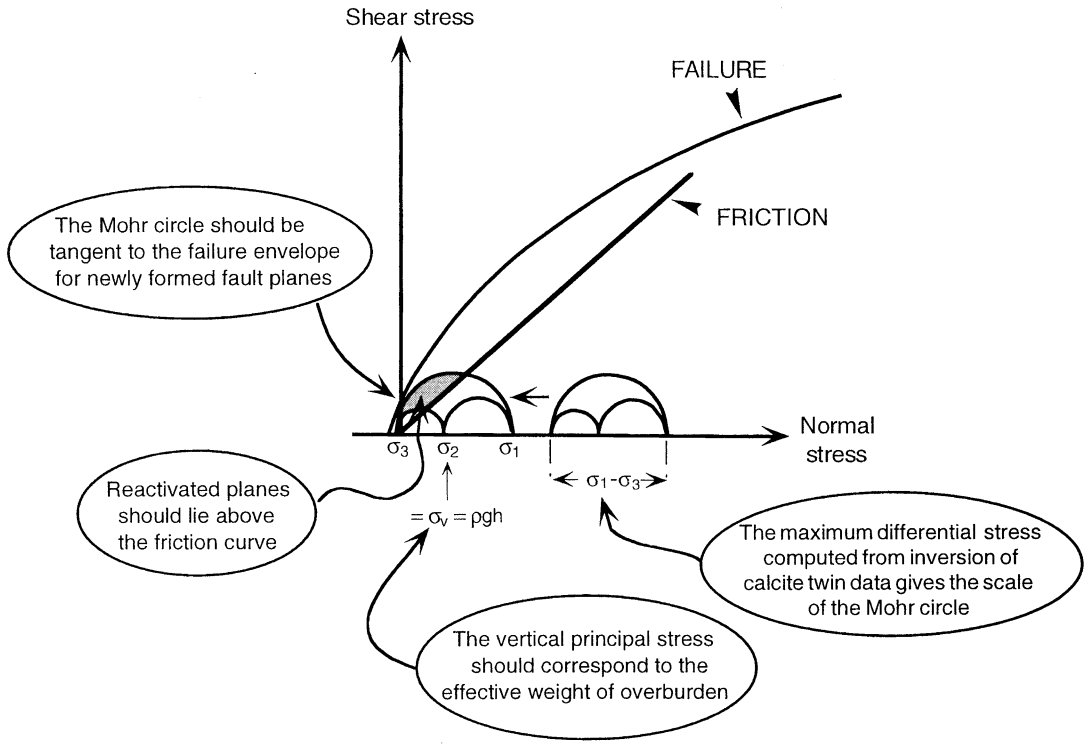

Figure 2. Principle of determination of principal stress magnitudes based on combination of inversion of calcite twin data, fracture analysis, paleodepth estimate and rock mechanics. Modified and completed after *Lacombe and Laurent* [1992].

differential stress magnitudes can be determined as follows [*Etchecopar*, 1984; *Lacombe and Laurent*, 1996; *Laurent et al.*, 2000]:

$$(\sigma_1-\sigma_3) = \tau_a / \tau_{a'} \quad \text{and} \quad (\sigma_2-\sigma_3) = \Phi(\sigma_1-\sigma_3),$$

where $\tau_{a'}$ is the smallest resolved shear stress applied on the twinned planes accounted for by the stress tensor and therefore the normalized value of the CRSS when $(\sigma_1-\sigma_3)$ is scaled to 1 (see section 2.1). Note that, as for other techniques of paleostress estimation based on calcite twin analysis [e.g., *Jamison and Spang*, 1976; *Rowe and Rutter*, 1990], the paleopiezometric technique used herein yields, for a given palaeostress orientation, the peak differential stress $(\sigma_1-\sigma_3)$ attained during the tectonic history of the rock mass, because the differential stresses are computed by taking into account the maximum percentage of twinned planes consistent with the tensor and therefore the smallest $\tau_{a'}$ value. Occurrence of a very low number of untwinned planes (< 10-15% of the whole data set) due, for instance, to polyphase tectonism may lead to underestimated $\tau_{a'}$ values and hence to overestimated $(\sigma_1-\sigma_3)$ values. The existence of such a bias toward high values when the number of untwinned planes is not sufficient has led to discard two samples from the Kaohsiung province (see section 4) where abnormally high differential stress values (larger than 300 MPa, that is, 5 to 10 times larger than the values determined from the neighboring samples) were obtained [*Rocher*, 1999].

The parameters of the deviatoric stress tensor T_D can therefore be determined as follows:

$$\sigma_{1D} = (2-\Phi)(\sigma_1-\sigma_3)/3 \qquad \sigma_{2D} = (2\Phi-1)(\sigma_1-\sigma_3)/3$$
$$\sigma_{3D} = -(1+\Phi)(\sigma_1-\sigma_3)/3$$

As a result, a single parameter is missing in defining the complete stress tensor. This sixth parameter corresponds to the isotropic component of the tensor that cannot be determined using calcite twinning only since twinning does not depend on isotropic stress. In order to assess the actual magnitudes of σ_1, σ_2 and σ_3, it is thus necessary to fix directly one of them, or at least to determine a third additional relationship between them.

2.3. Quantifying the Complete Stress Tensor

The method used herein to determine the complete stress tensor relies upon combination of analyses of calcite twins and rock mechanics data. This method, set out in detail by *Lacombe and Laurent* [1992], is only summarized here. For a given tectonic event and a given site, it consists of finding the values of σ_1, σ_2, and σ_3 required for compatibility between newly formed faulting, frictional sliding along preexisting planes, and calcite twinning. The theoretical principle of our technique is illustrated graphically in Figure 2.

2.3.1. Determination of principal stress magnitudes. The differential stress value $(\sigma_1-\sigma_3)$ determined from calcite twins fixes the scale (i.e., the diameter) of the Mohr circle associated with the tensor. To completely describe the stress regime (orientation and magnitude), the isotropic component of the tensor is missing. The determination of this parameter, which corresponds to the position of the Mohr circle along the normal stress axis in the Mohr diagram, can be done in the following ways.

2.3.1.1. Evaluation of the vertical stress: Paleostress determinations based on fault slip data and calcite twin data in platforms as well as in mountainous areas generally yield a highly plunging principal stress axis, close to vertical (within the usual 10°-15° range of uncertainties), provided that passively rotated stress axes due to folding are interpreted after backtilting to their

prefolding attitude (e.g., discussion in *Angelier* [1994]). In contrast, results of in situ measurements of present-day stresses show that the vertical stress is principal in regions of no topography and where rocks are either homogeneous or layered parallel to the ground surface, but that it is generally not the case in mountainous regions of significant topography and where geological structures are strongly developed (see discussion by *Goodman* [1989] and *Amadei and Stephansson* [1997]). A possible explanation of this difference is that paleostress reconstructions deal with stresses associated with tectonic deformation and hence of larger magnitudes and of longer duration (the duration of a tectonic event) than present-day stresses. These paleostresses are consequently "averaged" over several millions years, so they are controlled to the first order by the vertical (gravity) and the horizontal (tectonic forces) directions and do not reflect local and/or temporal sources of stress perturbation as the evolving-with-time topography can be. Consequently, since our analyses yield in most cases a nearly vertical principal stress, the magnitude of this vertical principal stress equals the effective weight of overburden as a function of the paleodepth of deformation. The actual pore fluid pressure at the time of deformation (and the porosity as well) being out of reach, hydrostatic conditions have been adopted hereinafter as the most realistic conditions of fluid pressure within the Plio-Quaternary Taiwanese reef limestones analyzed. In contrast, adopting dry conditions leads to maximum values of the vertical stress [*Angelier*, 1989].

2.3.1.2. Failure: If subsets of newly formed faults and twins provide similar reduced stress tensors in a given site, it can be reasonably inferred that they formed during the same tectonic event, and therefore they may be thought to have developed "contemporaneously" in terms of geologic time. As calcite twins record the "peak" stress reached during the entire history of the rock mass, the maximum recorded differential stress should correspond to the stress which induced rock failure, because fresh failure releases stress. Consequently, if new faults developed, fitting the (σ_3,σ_1) Mohr circle determined from calcite twins with the intrinsic failure (or crack development) curve yields values of principal stresses that prevailed just before rupture.

2.3.1.3. Friction: Because all points that represent reactivated preexisting planes should lie above the friction curve [*Byerlee*, 1978] in the Mohr circle, fitting the (σ_3,σ_1) Mohr circle determined from calcite twins with the friction line, so that inherited faults are located above the friction line, allows determination of the principal stress values. This requirement imposes a constraint on the position of the Mohr circle along the normal stress axis and yields principal stress magnitudes.

2.3.2. Determination of intrinsic curves corresponding to rupture. The intrinsic envelopes corresponding to failure and crack development within the limestone samples analyzed were determined using rock mechanics experiments. Samples (2.5 cm diameter and 5 cm length) were submitted to tension and to uniaxial compression under various confining pressures (0, 10, and 25 MPa); the magnitude of the deviatoric stress that must be applied to reach crack development (dilatancy) then macroscopic rock failure was evaluated. In the following sections, only the crack development curves that represent fracture development in natural conditions (including lithological heterogeneities and prefracturing) better than failure of fresh samples in the laboratory [e.g., *Bergerat et al.*, 1985] will be considered.

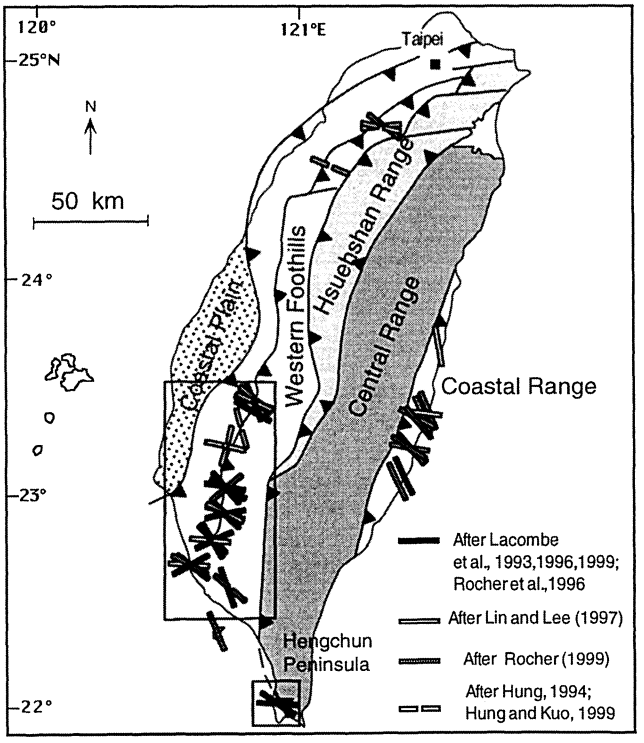

Figure 3. Plio-Quaternary stress orientations deduced from calcite twins within Neogene limestones in the Western Foothills and the Coastal Range of Taiwan. The frames show the areas investigated.

3. Sampling the Plio-Pleistocene Limestones in SW Taiwan

Figure 3 summarizes the results of paleostress reconstructions carried out since 1993 in Taiwan based on calcite twin analysis [*Lacombe et al.*, 1993, 1996; *Hung*, 1994; *Rocher et al.*, 1996; *Lin and Lee*, 1997; *Hung and Kuo*, 1999]. The mean stress orientation deduced from calcite twinning within Neogene limestones corresponds to the WNW-ESE to NW-SE compression which prevailed during the Plio-Quaternary and which controlled the emplacement of the major fold-thrust units [*Lacombe et al.*, 1999]. In SW Taiwan, however, a more recent E-W compression has also been identified. This is consistent with incipient right lateral motion along NNE thrusts and can be correlated with the onset of the present-day tectonic escape of the SW Taiwan area toward the SW [Lacombe et al., 1999].

Among the localities where the orientations of the Plio-Pleistocene stresses were reconstructed from Neogene limestones are the Kaohsiung and the Chukou areas (Figure 4a) where estimates of stress magnitudes have been obtained. These reef formations probably developed on structural highs raised by folding [e.g., *Gong et al.*, 1996; *Lacombe et al.*, 1999], on top of which decreasing clastic flow induced a local favorable paleoecological environment for reef building organisms (Figures 4b and 4c).

The Kungtien Pliocene (Nannoplankton zones NN14-NN15) limestone crops out in the Chukou area (Figure 4a); it consists of a subvertical carbonate lens interbedded within the Niaotsui formation (lower-middle Pliocene) on the eastern flank of the Chunglun anticline (Figure 4b). This Pliocene limestone was probably buried by 1500 m to 2500 m of sediments as estimated by the thickness of the upper Pliocene and Pleistocene sediments in this area [*Ho*, 1986](Figure 4b).

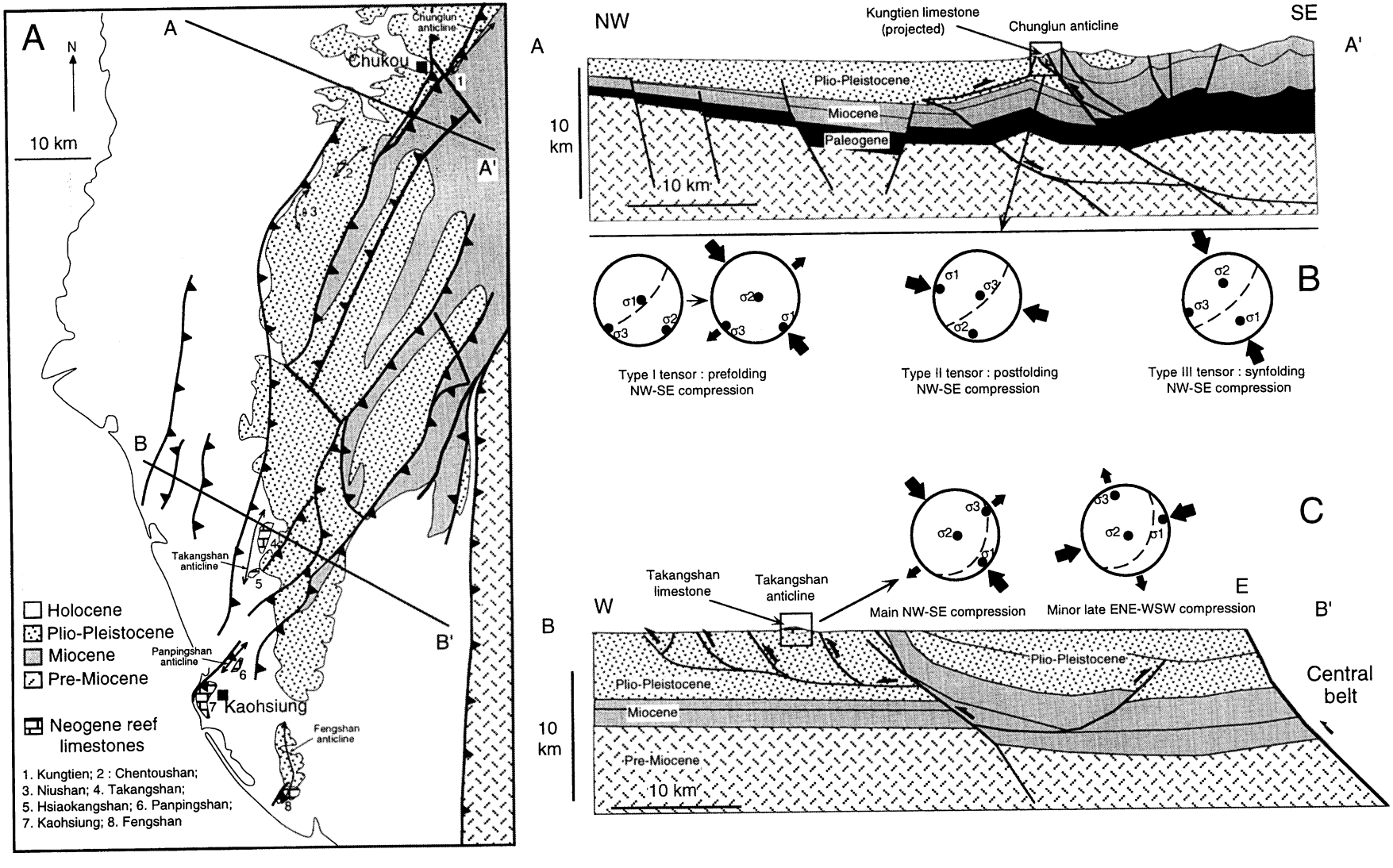

Figure 4. (a) Schematic structural map of SW Taiwan (location in Figure 3) showing the main thrust units and the outcropping formations. The limestone outcrops are labeled 1 to 8. (b) Balanced cross section in the Chukou area across the Chunglun anticline [*Mouthereau et al.*, 2001b] and types of stress tensors related to the NW-SE compression deduced from analysis of calcite twins. Bedding is shown on stereonets as a dashed line. The Kungtien limestone has been projected on the section. Note the involvement of the pre-Miocene formations and the superimposed shallow and deep-seated décollement tectonics. (c) Balanced cross section in the Kaohsiung area across the Takangshan anticline [*Mouthereau et al.*, 2001b] and stress tensors related to NW-SE and ENE-WSW compressions deduced from analysis of calcite twins. Note that most of deformation in the western part of the section occurs above a shallow decollement; regularly spaced thrusts and pop-up structures additionally indicate low-friction conditions.

Limestone formations of early Pleistocene age (NN19 Nannoplankton zone) crop out in the Kaohsiung area as large lenses of coarse crystalline limestones generally found interbedded within the shaly Gutingkeng formation. Samples were collected on the eastern flanks of the Takangshan anticline (Takangshan and Hsiaokangshan hills) and the Panpingshan anticline (Panpingshan and Kaohsiung hills) (Figure 4c), where reefal limestones display a shallow dip of 10°-20° to the ESE. The quaternary reefs of the Kaohsiung area were probably never buried by more than 300-400 m of sediments [*Gong et al.*, 1996].

Late Pleistocene limestones (NN20 Nannoplankton zone) were also collected on the western flank of the Fengshan anticline [*Lacombe et al.*, 1999](Figure 4a) as well as in the Kenting platform in the Hengchun peninsula [*Rocher et al.*, 1996](Figure 3).

At all of these localities, limestone samples were collected away from major fault zones where the stress field is known to be very inhomogeneous in both orientation and magnitude. The calcite twin-based paleostress reconstructions reported herein therefore meet the assumptions of stress homogeneity and low-finite strain and likely yield the regional paleostresses of interest.

This collection of Plio-Pleistocene limestone samples was complemented by sampling the recently uplifted Holocene reef platform along the shoreline in the Hengchun peninsula. These samples show no mechanical twinning [*Rocher et al.*, 1996; *Hung and Kuo*, 1999], so they can be treated as reference samples in which stresses were not sufficient to cause twinning.

4. Results

4.1. Stress Magnitudes Associated With the Development of the Chunglun Anticline (Chukou Area; Yutengping Site)

Three samples have been collected in the Kungtien limestone. Inversion of twin data from these samples yields various types of stress tensors, with σ_1 axes highly oblique (N110° to N160°) to the N020°E trending fold axis, but either parallel to bedding (type I tensors), or horizontal (type II tensors), or slightly dipping but less than the bedding dip (type III tensors)(Table 1). All the samples display polyphase twinning strain and have therefore provided at least two superimposed stress tensors that belong either to the same or to different types (I, II, and/or III). These geometrical relationships between stress axes and bedding (Figure 4b) have led *Lacombe et al.* [1996] to interpret type I tensors as prefolding tensors and type II as postfolding tensors. The type III probably corresponds to a twinning event contemporaneous with the latest stage of folding, but rotation of twins at the grain scale due to flexural slip [*Harris and Van der Pluijm*, 1998] cannot be definitely excluded.

Samples from the Chukou area show a high density of thin twin lamellae which sometimes display bending due to r gliding (Figure 5a), indicating an amount of low temperature strain of ~3.5% (mean twinning strain of 3.9% as deduced from reduced positive expected values obtained using *Groshong*'s analysis [*Hung and Kuo*, 1999]). So, on the basis of the new results shown in Figure 1, a CRSS of 12 MPa was adopted rather than the 10 MPa value previously used by *Lacombe et al.* [1996]. The differential stresses were consequently reevaluated as follows: For type I tensors, $(\sigma_1-\sigma_3)$ magnitudes range from 85 to 210 MPa (Table 1), with a weighted average value of 145 (± 50) MPa; for type II tensors they range from 54 to 76 MPa (Table 1) with a mean value of 65 (± 12) MPa; for the type III tensors they range from 52 to 85 MPa with a weighted mean value of 70 (± 14) MPa. Note that the stress tensors prevailing in the late stage of folding (type III) and the postfolding tensors (stage II) show the same small range of differential stress values, suggesting nearly homogeneous stress conditions since the late stages of folding; in contrast, the prefolding differential stress magnitudes show a large range of values, which probably reflects rapid changes in depth of overburden due to early synfolding exhumation and subsequent rapid changes in differential stress magnitudes.

The technique previously described in section 2, which combines the analysis of calcite twins and rock mechanics data, provides orders of magnitudes associated with the NW-SE compression. Oscillations between strike-slip and reverse faulting [*Lacombe et al.*, 1996] suggest that the magnitudes of σ_2 and σ_3 were close one to each other. Fitting the (σ_3,σ_1) Mohr circles of diameters 145 MPa and 70 MPa to the average crack development

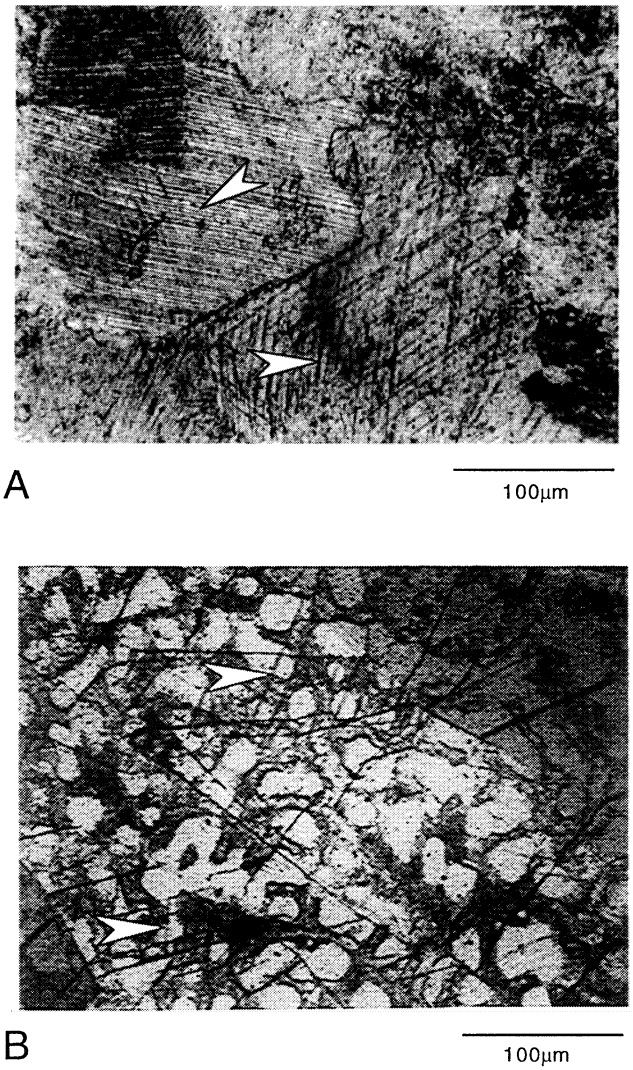

Figure 5. (a) Microphotograph (natural light) of the Kungtien reef limestone showing thin twin lamellae (arrows). Note the high twin density and the occurrence of twin bending due to r gliding. (b) Microphotograph (natural light) of the Takangshan reef limestone showing thin twin lamellae (arrows) cutting through sparry calcite crystals resulting from recrystallization regardless of the initial coralline organic network. In contrast with Figure 5a, the twin density is low.

Table 1. Characteristics of Compressional/Strike-Slip Stress Tensors Computed From Calcite Twin Data in the Chukou, Kaohsiung, Fengshan, and Kenting Areas and Used for Stress Estimates[a]

Sample Number	Type of the State of Stress	Trend-Plunge of the Principal Stress Axes, degrees						Ratio Between Differential Stresses, Φ	Function of Minimiza--tion, f	Number of Twinned Planes	Number of Untwinned Planes	Twinned Planes Consistent	Untwinned Planes Unconsistent	σ1-σ3 Value, MPa
		σ1		σ2		σ3								
								Fengshan Area						
S1	E-W comp	160	16	070	10	339	74	0.2	0.5	83	14	24	1	23
								Chukou Area (Yutengping Site)						
S1	NW comp I	134	11	277	77	042	8	0.5	0.00	252	24	93	0	210
	NW comp I	333	12	074	38	229	48	0.6	0.10	96	23	48	2	143
	NW comp II	136	0	226	6	046	84	0.4	0.00	159	23	63	0	76
S2	NW comp I	154	23	039	44	264	37	0.8	0.30	171	28	68	3	85
	NW comp II	286	1	195	6	028	84	0.4	0.04	227	22	56	1	54
S3	NW comp III	312	39	213	11	110	49	0.3	0.12	171	31	76	3	77
	NW comp III	288	24	122	66	020	5	0.0	0.11	96	30	28	2	85
	NW comp III	164	37	248	53	256	2	0.3	0.13	68	30	27	6	52
								Kaohsiung Area (Takangshan Site)						
S1	NW comp	340	23	211	55	81	24	0.7	0.25	173	26	79	5	107
	E-W comp	100	9	193	21	348	67	0.3	0.32	53	20	40	5	28.5
S2	NW comp	121	17	248	64	25	20	0.2	0.14	206	22	92	3	71
								Kaohsiung Area (Hsiaokangshan Site)						
S1	E-W comp	79	17	262	73	169	1	0.2	0.03	127	25	60	2	36.5
	NW comp	316	2	54	73	226	17	0.6	0.21	71	24	30	2	33
S2	NW comp	289	2	198	19	25	71	0.2	0.18	173	63	57	1	25
	E-W comp	79	33	245	56	344	6	0.5	0.40	116	63	34	5	21
								Kaohsiung Area (Panpingshan Site)						
S1	NW comp	133	2	350	88	223	1	0.5	1.02	179	38	98	7	110
	E-W comp	67	22	167	22	297	57	0.5	0.79	54	36	37	8	29
S2	NW comp	150	26	307	62	56	10	0.6	0.00	97	16	43	0	62
	E-W comp	69	1	339	19	163	71	0.4	0.00	55	15	26	0	20
								Kaohsiung Area (Kaohsiung Site)						
S1	NW comp	134	26	344	61	230	13	0.4	0.08	84	20	37	2	25
	E-W comp	243	4	148	55	335	35	0.2	0.06	47	20	18	2	28.5
S2	E-W comp	242	4	333	13	135	76	0.6	0.15	109	62	35	3	15
								Kenting Area (Hengchun Site)						
S1	E-W comp	93	1	303	89	183	0	0.5	0.00	36	14	18	0	24
	NW comp	304	6	166	81	34	6	0.2	0.17	18	15	12	2	33

[a]Extensional stress tensors also determined from the sites investigated have not been reported. Data on stress tensors are from *Lacombe et al.* [1993, 1996], *Rocher et al.* [1996], and *Rocher* [1999]. Differential stress estimates are based on τ_a determinations (see text for details) from *Lacombe et al.* [1996] and *Rocher* [1999]. For the Chukou area (Chunglun anticline), I, II and III refer to types of stress tensors defined in Figure 4b; for type I tensors, stress axes are in their backtilted attitude (i.e., after rotation of the bedding along its strike).

curve (Figure 6) leads to values of principal stresses of $\sigma_1 \sim 175$ MPa and $\sigma_2 \sim \sigma_3 \sim 30$ MPa for prefolding stresses and $\sigma_1 \sim 80$ MPa and $\sigma_2 \sim \sigma_3 \sim 10$ MPa for synfolding and postfolding stresses, respectively.

Following *Harris and Van der Pluijm* [1998], this study emphasizes that twinning may occur both before folding as layer-parallel shortening (LPS) passively tilted as folding occurs [*Craddock and Van der Pluijm*, 1989; *Ferrill and Groshong*, 1993b], after fold development [*Groshong et al.*, 1984; *Rowe and Rutter*, 1990], and during folding [*Ferrill and Groshong*, 1993a]. However, the limited evidence of synfolding twinning suggests that twinning strain is mainly achieved during the early and late stages of folding, probably during two peaks of stresses which seem to predate immediately folding (buckling) and to prevail after fold tightening [*Onasch*, 1983].

Although the Chunglun anticline is rather complex, a simplified tectonic history can be drawn for the time-spatial relationships between stresses inferred from twins (and from fault slip data [*Lacombe et al.*, 1996]) and fault propagation folding (Figure 6a). First, twinning strain occurs (type I tensors) in association with

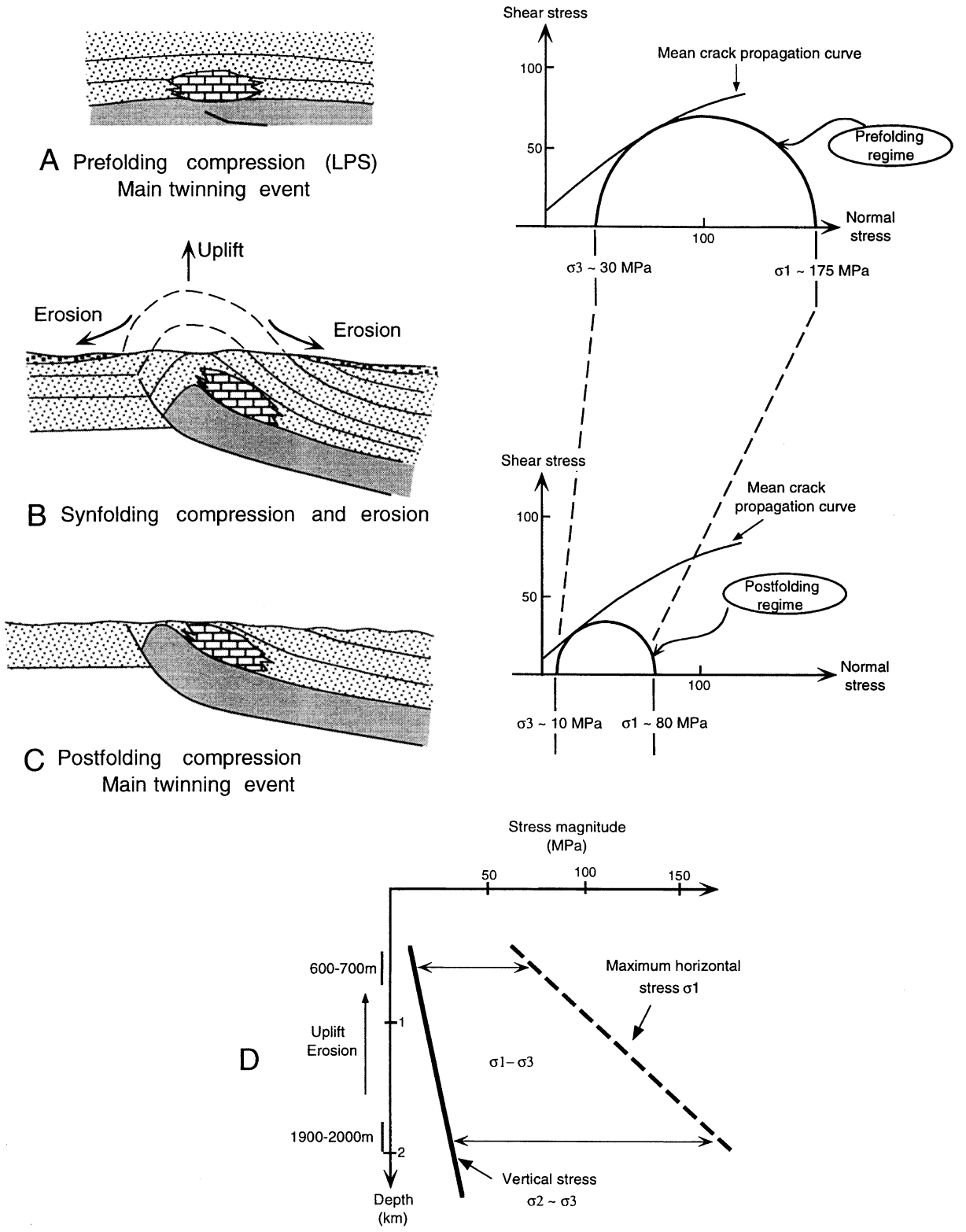

Figure 6. (a-c) Simplified tectonic model of fault-related fold development showing contemporaneous evolution of stress magnitudes based on the results from the Chunglun anticline. (d) Inferred evolution of stress magnitudes with depth. Note the decrease of differential and principal stress values related to synfolding erosion and subsequent exhumation. LPS, layer-parallel shortening.

minor faulting and pressure solution, before or during the onset of folding (LPS); it corresponds to mixed compressional and strike-slip stress regimes, under an average NW-SE compression and high levels of differential stresses (Figure 6a). The travel along the ramp and the related transport is associated with shortening oblique to bedding, leading to mixed pure shear (recorded by twinning; type III tensors ?), and simple shear (bedding-parallel slip, as deduced from slickensides observed in the field along beds) deformation; fold development caused rapid uplift and subsequent erosion (Figure 6b), leading to both rapid decreasing lithostatic load and differential stresses during the early stages of folding. Finally, because of locking of the thrust, the whole system is homogeneously shortened, and late twinning occurs (type II tensors) under lower stress levels (Figure 6c).

Equaling the magnitude of the calculated vertical stress $\sigma_2 \sim \sigma_3$ with the effective weight of overburden $[(\rho-\rho_e)gh$, with g the acceleration of gravity] consequently suggests a cover thickness h of about 1900-2000 m before folding and 600-700 m after folding if an average rock density ρ of 2600 kg/m^3 and hydrostatic conditions (water density ρ_e of 1000 kg/m^3) are assumed. These estimates are consistent with stratigraphic data [*Ho*, 1986] indicating at least 1500 m of late Pliocene sediments above the studied formation in the area investigated at the time of deformation. They also suggest a synfolding erosion of ~1000-1200 m during the Pleistocene NW-SE compression (Figure 6d).

4.2. Stress Magnitudes Associated With the Development of the Takangshan and Panpingshan Anticlines (Kaohsiung Area; Takangshan, Hsiaokangshan, Panpingshan, and Kaohsiung Sites)

The reef limestones which crop out in Takangshan, Hsiaokangshan, Panpingshan and Kaohsiung localities (Figure 4a) have been studied in great detail using calcite twins both in terms of stress [*Lacombe et al.*, 1993; *Rocher et al.*, 1996] and strain [*Hung and Kuo*, 1999] orientations. The results of paleostress reconstruction using the twin inversion technique are summarized in Figure 4c. Two compressional stress regimes have been identified: a NW-SE compression, followed by an E-W compression. The NW-SE compression is associated with the major stage of fold development and related reef building; the ENE-WSW to E-W compression mainly prevailed during the latest stages of folding. Note that these stress regimes have been identified independently using fault slip analysis [*Lacombe et al.*, 1999].

Calcite twin analyses carried out from samples collected in the early Pleistocene limestones (two samples at each locality) provide information about the stress levels that prevailed during the Quaternary development of outer folds in the western Taiwan Foothills. The low density of thin straight twin lamellae observed within the samples from the Kaohsiung area (Figure 5b) indicates a low amount of strain (mean twinning strain of 2% as deduced from reduced positive expected values obtained using *Groshong*'s analysis [*Hung and Kuo*, 1999]). I consequently adopted a CRSS of 5 MPa (see Figure 1) for the calculation. For the major NW-SE compression which prevailed contemporaneous with folding [*Lacombe et al.*, 1999], the magnitudes of the differential stress $(\sigma_1-\sigma_3)$ range from 25 MPa to 110 MPa (Table 1); the weighted average value of ~ 60 (± 35) MPa is probably the most realistic estimate of the regional stress magnitudes. Note that the bedding dip is too low to allow unambiguous identification of prefolding, synfolding and postfolding stress tensors corresponding to the NW-SE compression; however, this bedding dip may explain the slight obliquity of reconstructed principal stress axes (Table 1). For the late ENE-WSW to E-W compression which prevailed after folding [*Lacombe et al.*, 1999], the magnitudes of the differential stresses $(\sigma_1-\sigma_3)$ are much more homogeneous and range from 15 MPa to 37 MPa, with a weighted average value of ~ 26 (± 10) MPa.

As before, because newly formed faults related to both NW-SE and E-W compressions have been identified, estimates of orders of magnitude of stresses can be obtained by fitting the (σ_3,σ_1) Mohr circles of diameters 60 MPa and 26 MPa to the average crack propagation curve (Figure 7). The same curve has been used for all localities of the Kaohsiung area since the limestone samples from Takangshan, Hsiaokangshan, Panpingshan, and Kaohsiung display similar petrographic characteristics. Average values of principal stresses of $\sigma_1 \sim 65$ MPa and $\sigma_2 \sim \sigma_3 \sim 5$ MPa for the NW-SE compression and $\sigma_1 \sim 26$ MPa and $\sigma_2 \sim \sigma_3 \sim 0$ MPa for the late E-W compression, respectively, are obtained (Figure 7). As the Pleistocene limestones of the Kaohsiung area have never been significantly buried [*Gong et al.*, 1996], the thickness of overlying sediments very probably never exceeded 300-400 m. This is consistent with the paleodepth of deformation that can be deduced from our results assuming the same effective weight of overburden than before.

4.3. Stress Magnitudes in the Fengshan and Kenting Areas

In each of these areas a single sample of late Pleistocene limestones has yielded significant results. This observation is consistent with the bad quality of results obtained by *Hung and Kuo* [1999] in the Hengchun peninsula, where the estimated strain averages 1.8% (mean twinning strain deduced from reduced positive expected values obtained using *Groshong*'s analysis).

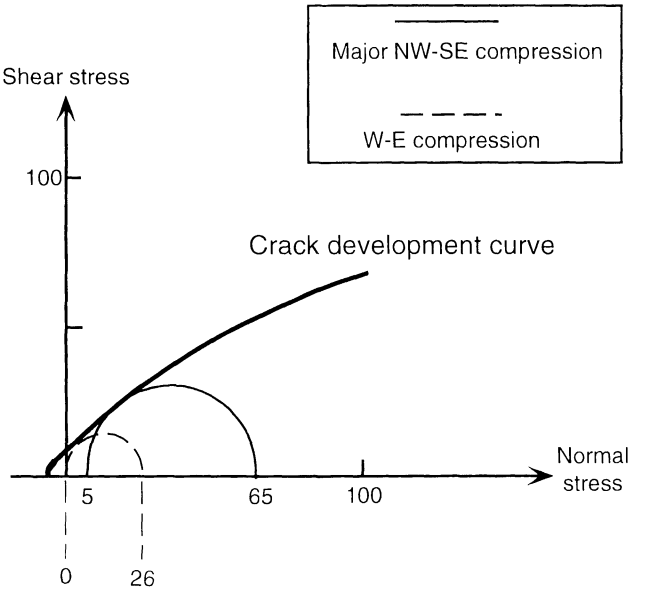

Figure 7. Principal stress values associated with the NW-SE and the E-W compression in the Kaohsiung province. The diameters of the Mohr circles correspond to the average differential stress values deduced from inversion of calcite twin data for each stress regime. Fitting the Mohr circles with the crack development curve (heavy line) determined from laboratory experiments is justified since newly formed faults developed under both stress regimes (for details, see text). Stress values are in MPa.

The differential stress value (σ_1-σ_3) corresponding to the WNW-ESE to E-W compression obtained at Fengshan is 23 MPa (Table 1). Fitting the corresponding Mohr circle with the average crack development curve determined for the early Pleistocene limestones leads to rough estimates of σ_1 and σ_3 values of ~23 MPa and 0 MPa, respectively. The NW-SE compression has not been identified [*Lacombe et al.*, 1999].

At the Kenting locality in the Hengchun peninsula, both the NW-SE and the E-W compressions have been identified [*Rocher et al.*, 1996]. Differential stress estimates yield a 33 MPa value for the NW-SE compression, and they yield a 24 MPa value for the E-W compression (Table 1). A noticeable thing is that no fracture or striated microfault has been observed where the sample was collected, so that fitting the Mohr circle determined from calcite twins with the average crack development curve was not theoretically justified. As a result, the only way to determine principal stress magnitudes (Figure 1) consists of evaluating the burial depth which was close to 0, which provides σ_1 and σ_3 values of ~ 33 MPa and 0 MPa for the NW-SE compression and ~24 MPa and 0 for the E-W compression.

5. Discussion

5.1. Uncertainties on the Determination of Paleostress Magnitudes Using the Twin Inversion Technique

The stress estimates reported in this paper show a large scatter around the weighted mean values (Table 2). Possible explanations lie in both the complexity of natural settings and the intrinsic limitations of the technique used to infer paleostresses. In addition to local structural inhomogeneities some natural aggregates display very inhomogeneous distribution of grain size and grain shape, so local stress inhomogeneities at the thin section scale may occur and influence the estimated differential stress magnitudes. On a technical point of view, estimates of differential stress magnitudes are based on the accurate determination of the τ_a value, which depends on both the percentage of twinned planes included in the solution and the percentage and spatial distribution of untwinned planes. If twinning results from superimposed stress tensors, the number of untwinned planes can be low (<10% of the whole data set), so stress magnitudes are much less constrained than for monophase tectonism: in this case, the variation of +/- 5% of twin data included in the solution may lead to uncertainties of ~30-50% on the differential stress values. The accurate definition of the optimal solution, based on both quality estimators (percentage of untwinned planes taken into account for calculation, value of the f function) and the stability of the calculated parameters of the tensor (orientation of stress axes, Φ ratio) is therefore a key point of the twin inversion technique; this aspect has been discussed elsewhere by *Lacombe and Laurent* [1996] and *Laurent et al.* [2000] on the basis of the inversion of calcite twin data from experimentally deformed samples.

As a consequence, taking into account the multiple sources of uncertainties, more or less shared by all the methods of stress estimates based on the calcite twinning paleopiezometry, only orders of differential stress magnitudes can be sought and reasonably inferred. Concerning the calculation of principal stress magnitudes, a main source of uncertainty lies in the estimate of the effective weight of overburden, which is the paleodepth of deformation and the pore pressure. The latter is of considerable importance for stress estimates, because (1) even though the frictional criterion has not been used in this paper to infer paleostresses, friction involves the effective normal stress and therefore the pore pressure magnitude, and the frictional strength of the upper crust depends largely on effective stresses, (2) in the absence of fault slip data, estimates of principal stress magnitudes rely upon the determination of the magnitude of the effective

Table 2. Orders of Magnitudes of Principal Stresses and Estimated Paleodepths of Deformation in the Chukou, Kaohsiung, Fengshan and Kenting Areas[a]

Type of the State of Stress	σ1-σ3 Value, MPa	Mean σ1 value, MPa	Mean σ2 ~ σ3 Value, MPa	Paleo-depth, m (Predicted)	Paleo-depth, m (Stratigraphy)
		Chukou Area			
NW comp I	145 ± 50 (3)	175	30	1900±300	1500 - 2500
NW comp II	65 ± 12 (2)	80	10	600±100	?
NW comp III	70 ± 14 (3)	80	10	600±100	?
		Kaohsiung Area			
NW comp	60 ± 35 (7)	65	5	300±50	< 400
E-W comp	26 ± 10 (7)	26	0	~ 0	~ 0
		Fengshan Area			
E-W comp	23 (1)	23	0	~ 0	~ 0
		Kenting Area			
E-W comp	24 (1)	24	0	-	~ 0
NW comp	33 (1)	33	0	-	~ 0

[a]Numbers in parentheses indicate the number of independent estimates (see Table 1). Paleodepth (predicted) refers to estimate derived from the vertical stress magnitude assuming hydrostatic conditions. Paleodepth (stratigraphy) refers to estimate based on stratigraphic data.

vertical stress that depends on fluid pressure, and (3) when principal stress magnitudes are determined by combining calcite twin data and fault slip data, predicting the paleodepth of deformation (to be compared to independent estimates using stratigraphic information) also requires the estimate of the magnitude of the effective vertical stress. In this paper, hydrostatic conditions have been adopted as the more likely fluid pressure conditions within the Plio-Quaternary reef limestones studied, and our samples have been located at depth accordingly (Table 2). However, uncertainties on this paleodepth may arise since in compression zones, pore pressure may be closer to lithostatic than to hydrostatic.

A possible future way to reduce the range of uncertainties on stress estimates could be to combine the use of tectonic stress indicators with the analysis of fluid inclusions, which allows the derivation of the pore pressure from the fluid density or inference of the value of the vertical stress assuming hydrostatic conditions [e.g., *Lespinasse and Cathelineau*, 1995]. In fold-thrust belts, estimates of paleodepth of deformation could be significantly constrained by the additional use of paleothermometers (such as vitrinite reflectance, illite crystallinity, or fluid inclusions) coupled with numerical modeling of the thermal evolution of tectonic units which has the potential to constrain the paleoburial.

5.2. Order of Magnitudes of Tectonic Stresses Associated With Development of the Taiwan Fold-Thrust Belt

All the samples examined have deformed under a thin-twin regime (Figure 5), suggesting that temperature never exceeded 200°C. In addition, mechanical twinning was associated with pervasive pressure solution coupled with mesoscale faulting (and sometimes bedding-parallel slip) associated with shear calcite fibers [*Lacombe et al.*, 1996, 1999], suggesting that these rocks mainly deformed with the elastic-frictional regime [*Elliott*, 1976].

The range of differential stress values determined for the regional NW-SE compression in Taiwan is ~ 60-140 MPa for samples deformed at depths between 300 m and 2000 m. At Chukou locality the decrease of differential stress values inferred from the comparison between prefolding and postfolding stages is probably due to the decreasing weight of overburden during synfolding erosion. The difference between the average differential stress value estimated for the postfolding stage at Chukou locality (~ 70 MPa) and that obtained in the Kaohsiung area (60 MPa) for the NW-SE compression could also be related to a different paleodepth of deformation. However, the same NW-SE compression is associated in the Hengchun peninsula with a value of differential stresses (23 MPa) much lower than in the Kaohsiung area: This difference cannot be accounted for only by the slight difference in paleodepth of deformation, and therefore it suggests a southward decrease in stress magnitudes.

Hung and Kuo [1999] recognized an overall southward (from Chukou to Hengchun) decrease in mean finite strain determined from the reef limestones. Since the age of these limestones also decreases southward [e.g., *Gong et al.*, 1996], they propose that the strain decrease reflects a longer application of stresses in older and, consequently, more deeply buried samples than in younger ones. A similar explanation can be proposed for the southward decrease in differential stress magnitudes provided that the depth of burial is an important parameter controlling differential stress values. However, the difference in stress magnitudes accompanying folding between the Chukou area and the southern Taiwan Foothills could also partly lie in the strong contrast of deformation styles between the two regions. As Figure 4b shows, the Chukou area belongs to an area where actual collision is taking place and where the pre-Miocene formations (including the crystalline basement ?) are involved in the deformation of frontal areas [*Mouthereau et al.*, 2001a]; in contrast, the southwestern province can be considered as the onland extension of the Manilla accretionary prism and deforms mainly above a low-dipping shallow décollement surface (Figure 4c)[*Lacombe et al.*, 1999]. I tentatively propose that involvement of the basement and occurrence of superimposed shallow and deep décollement tectonics [*Mouthereau et al.*, 2001b] in the frontal part of the Taiwan orogenic wedge in the Chukou area were associated with high-friction conditions which could have led to tectonic records of high stress levels in the rocks before folding occurred. This could be an explanation accounting for the higher levels of differential stresses accompanying folding in the Chukou area compared to the southern province made of thick poorly consolidated muddy Quaternary deposits where regularly spaced fault-propagation folds and pop-up structures indicate low-friction conditions [*Lacombe et al.*, 1999].

Concerning the late E-W compression, which was identified only in the Kaohsiung, Fengshan and Hengchun areas, the differential stress values are much lower and homogeneous (around 25 MPa). In contrast to the NW-SE compressional regime, which was clearly contractional and associated with the major stage of fold development, this second regime generally prevailed during the latest stages of folding in the southern province and was associated from north to south with an increasing component of perpendicular extension reflecting a southward decrease in N-S confinement. This nearly E-W (locally ENE-WSW) compression is consistent with an incipient right-lateral component of motion along NNE thrusts. It therefore supports a late Pleistocene onset of the tectonic escape that occurs at the present-day in SW Taiwan [*Lacombe et al.*, 1999]. The low differential stress magnitudes associated with this compression are consistent with the fact that no major structure (except the Fengshan anticline) developed under this "weak" compression and that faults were probably activated or reactivated due to local high fluid pressure.

6. Evolution with Depth of Stress Magnitudes in Compressional Settings

The results obtained in the present study partially fill a gap between stress estimates carried out in foreland and hinterland

Figure 8. (a) Schematic sketch showing that rocks which now crop out in foreland, fold-thrust and hinterland domains of orogens have been deformed at very different depths during crustal wedging and that the increase in differential stress magnitudes from the foreland toward the hinterland consequently mainly reflects increasing burial depth. (b) Differential stress versus depth (log-log) diagram. Modified and completed after *Davis and Engelder* [1985] and *Ferrill* [1998]. The two main stress-depth gradients identified (shaded) are labeled A and B. Taiwan Yutengping (a) and Taiwan Yutengping (b) refer to prefolding and postfolding stress values, respectively, in the Chukou area. Subalpine chain (a) and subalpine chain (b) refer to stress estimates carried out by *Ferrill* [1998] using the *Jamison and Spang* [1976] technique and the *Rowe and Rutter* [1990] technique, respectively.

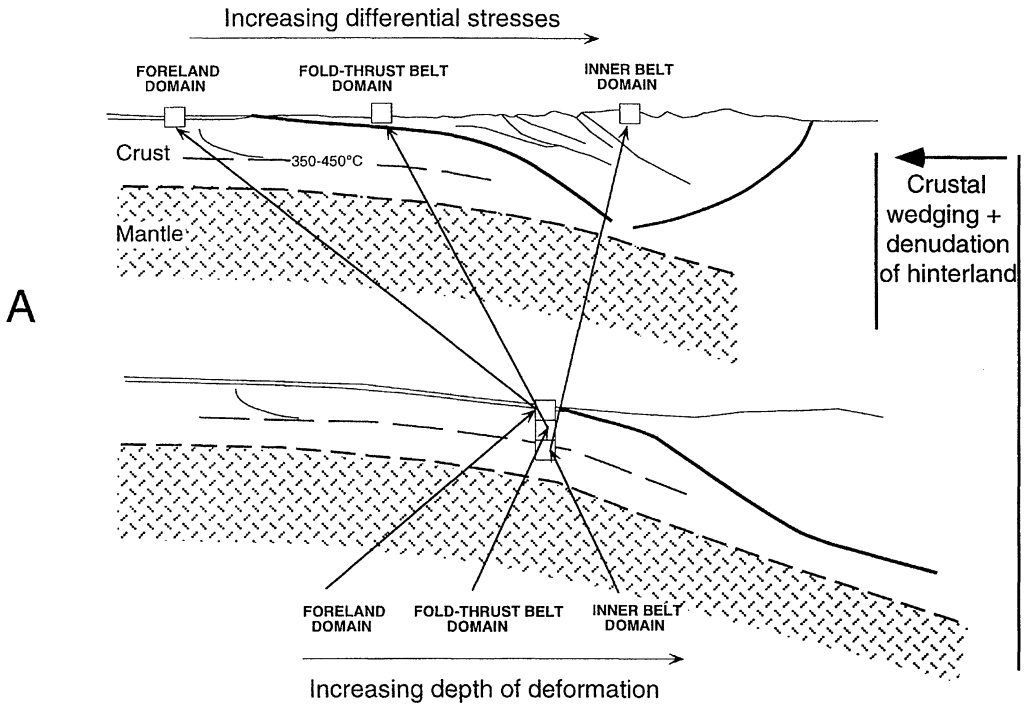
A
Increasing differential stresses
FORELAND DOMAIN
FOLD-THRUST BELT DOMAIN
INNER BELT DOMAIN
Crust
350-450°C
Mantle
Crustal wedging + denudation of hinterland
FORELAND DOMAIN
FOLD-THRUST BELT DOMAIN
INNER BELT DOMAIN
Increasing depth of deformation

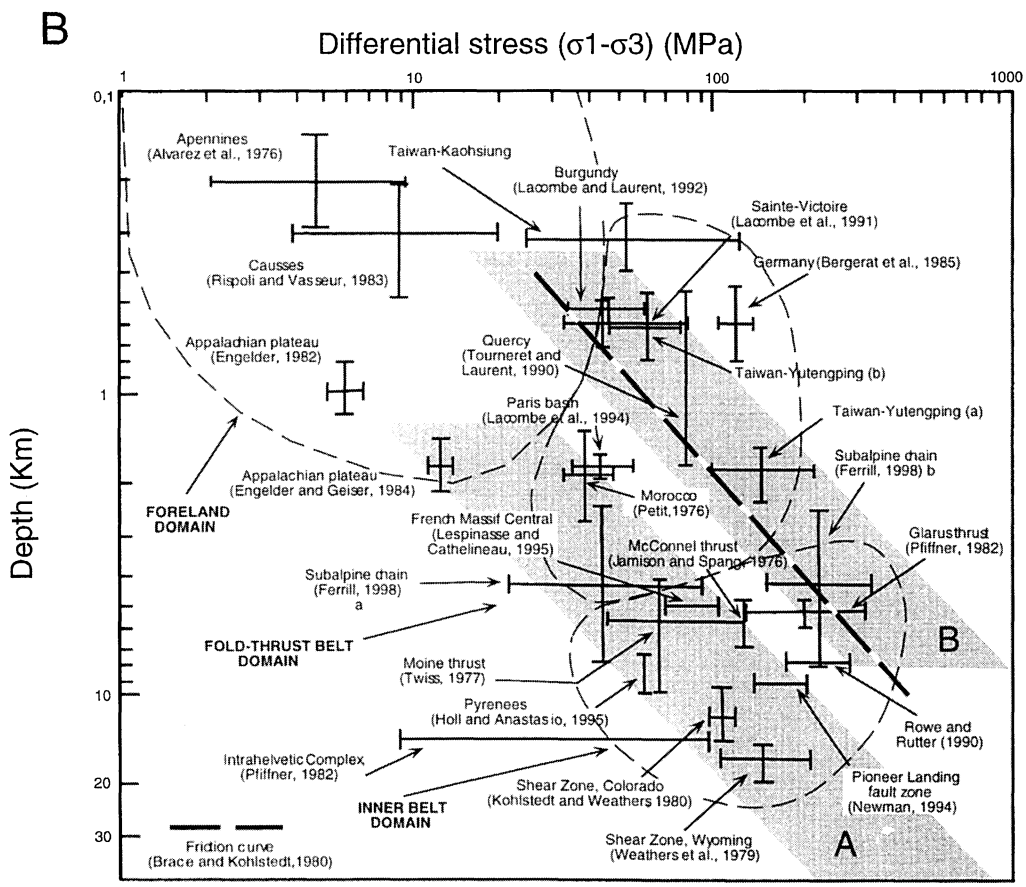
B
Differential stress (σ1-σ3) (MPa)
1
10
100
1000
0,1
1
10
20
30
Depth (Km)
Apennines (Alvarez et al., 1976)
Taiwan-Kaohsiung
Burgundy (Lacombe and Laurent, 1992)
Sainte-Victoire (Lacombe et al., 1991)
Causses (Rispoli and Vasseur, 1983)
Germany (Bergerat et al., 1985)
Appalachian plateau (Engelder, 1982)
Quercy (Tourneret and Laurent, 1990)
Taiwan-Yutengping (b)
Paris basin (Lacombe et al., 1994)
Taiwan-Yutengping (a)
Subalpine chain (Ferrill, 1998) b
Appalachian plateau (Engelder and Geiser, 1984)
FORELAND DOMAIN
Morocco (Petit,1976)
French Massif Central (Lespinasse and Cathelineau, 1995)
McConnel thrust (Jamison and Spang, 1976)
Glarusthrust (Pfiffner, 1982)
Subalpine chain (Ferrill, 1998) a
FOLD-THRUST BELT DOMAIN
B
Moine thrust (Twiss, 1977)
Pyrenees (Holl and Anastasio, 1995)
Rowe and Rutter (1990)
Intrahelvetic Complex (Pfiffner, 1982)
Shear Zone, Colorado (Kohlstedt and Weathers 1980)
Pioneer Landing fault zone (Newman, 1994)
INNER BELT DOMAIN
Shear Zone, Wyoming (Weathers et al., 1979)
A
Friction curve (Brace and Kohlstedt,1980)

Figure 8.

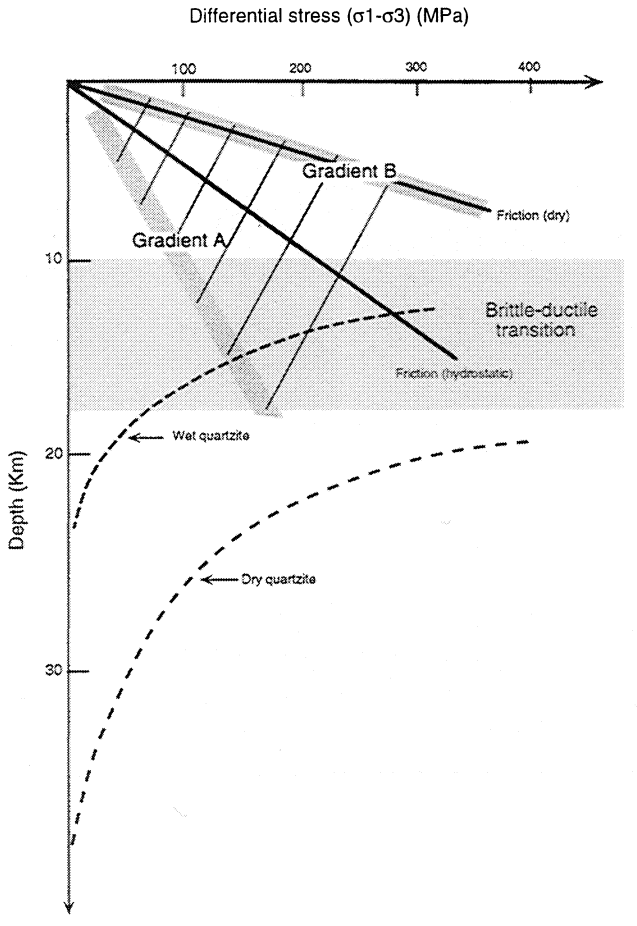

Figure 9. Evolution with depth of the strength of the upper continental crust deduced from stress and paleostress estimates from naturally deformed rocks. Hatched area corresponds to the range of obtained stress estimates. Friction curves are from *Brace and Kohlstedt* [1980]. Shaded area shows brittle-ductile transition. Note that stress data are consistent with a frictional behavior of the upper crust under hydrostatic conditions.

domains of orogens. Gathering the stress data available from literature about compressional settings suggests a trend of increasing differential stresses from the undeformed foreland toward the hinterland of mountain belts (Figure 8a).

As was already mentioned by *Newman* [1994], the difficulty met in comparison of stress estimates arises from the method dependence of estimates: Although the increase toward the hinterland may be real, estimates group according to the methods used. This method dependence is for instance illustrated in Figure 8b where stress estimates within the Subalpine Chain carried out by *Ferrill* [1998] using both the *Rowe and Rutter* [1990] method and the *Jamison and Spang* [1976] method have yielded very different results. In addition, estimates also group according to regional studies (forelands, fold-thrust belts) versus fault zones (inner belts) studies.

Recent works have documented an exponential decrease of orogenic stresses within the foreland of orogens up to 2500 km from the orogenic front [*Craddock et al.*, 1993; *Lacombe et al.*, 1996; *Van der Pluijm et al.*, 1997]. This decrease of differential stresses from 100 MPa close to the orogenic front to 10-20 MPa in the far foreland mainly reflects stress attenuation with increasing distance from the plate boundary because foreland rocks likely deformed at nearly similar depths. However, even though this effect may also apply at the scale of the entire orogenic system (Figure 8a), the increase of differential stresses from 10-20 MPa in the foreland to 200 MPa in the hinterland (Figure 8b) rather indicates an overall increase of differential stresses with depth since rocks now exposed at the surface in fold-thrust belts and metamorphic belts have deformed at much deeper crustal levels compared to foreland rocks during crustal wedging (Figure 8a). From the diagram of Figure 8b, where differential stresses are plotted against depth (log-log), three main stress-depth domains can be recognized: The foreland domain comprises mainly sedimentary rocks deformed at shallow depths (between nearly 0 and 2 km) under differential stress values between 5-10 and 40 MPa; the fold-thrust domain (where the present study takes place) includes both sedimentary and slightly metamorphosed rocks deformed at depths between 300 m and 4-5 km, under differential stress values between 30 and 140 MPa; the inner belt domain displays metamorphic rocks deformed at depths between 5 km and 15 km under differential stress values between 50 and 200 MPa. Defining the way differential stresses evolve with depth is not easy; however, the data lie between two stress-depth gradients (A and B in Figure 8b) that define the range of natural differential stress values at depth. The gradient B follows more or less the dry friction curve of *Brace and Kohldsted* [1980]. The overall increase of differential stress magnitudes with depth reflects that tectonic stresses are much less easily released at depth because of the increasing pressure up to 15 km. This is consistent with the brittle rheology of the upper crust obeying Byerlee's friction law [*Brace and Kohldsted*, 1980](Figure 9).

The data of Figure 8b effectively support the behavior of the upper crust as predicted by the rheologic envelopes of the continental crust (Figure 9). A fluctuating brittle-ductile transition (350°-450°C ?) must be defined depending on the geotherm and therefore of the settings where stress estimates in fault zones have been performed in order to reconcile occurrence within these fault zones of ductile deformation processes and high stress levels rather consistent with frictional rheology. Taking this transition into account, the data of Figure 8b are consistent with a frictional behavior of the upper crust (Figure 9). They independently support that the mechanical strength of the upper continental crust away from plate boundaries is governed by friction law with friction coefficient of 0.6-0.9 assuming a nearly hydrostatic fluid pressure [*Brudy et al.*, 1997] and is limited by the frictional strength on preexisting favorably oriented faults [*Zoback et al.*, 1993]. As a result, the brittle upper continental crust is able to sustain differential stresses probably as large as 150-200 MPa, so its strength makes it able to transmit a significant part of orogenic stresses from the plate boundary toward the far foreland.

Acknowledgments. The author would like to thank the two reviewers, F. Cornet and B. Van der Pluijm, as well as the European Editor F. Roure for their constructive comments, which allowed the manuscript to be improved.

References

Alvarez, W., T. Engelder, and W. Lowrie, Formation of spaced cleavage and folds in brittle limestone by dissolution, *Geology*, *4*, 698-701, 1976.

Amadei, B., and O. Stephansson (Eds.), Rock Stress and Its Measurements, pp. 51-61, Chapman and Hall, New York, 1997.

Angelier, J., Tectonic analysis of fault slip data sets, *J. Geophys. Res.*, *89*, 5835-5848, 1984.

Angelier, J., From orientation to magnitudes in paleostress determination using fault slip data, *J. Struct. Geol*, *11*, 37-50, 1989.

Angelier, J., Fault slip analysis and paleostress reconstruction, in *Continental Deformation*, edited by P. Hancock, pp. 53-100, Pergamon, New York, 1994.

Bergerat, F., J. Bergues, and J. Geyssant, Estimation des paléocontraintes liées à la formation de décrochements dans la plate-forme d'Europe du Nord, *Geol. Rundsch.*, *74*, 311-320, 1985.

Brace, W.F., and D.L. Kohlstedt, Limits on lithospheric stress imposed by laboratory experiments, *J. Geophys. Res.*, *85*, 6248-6252, 1980.

Brudy, M., M.D. Zoback, K. Fuchs, F. Rummel, and J. Baumgärtner, Estimation of the complete stress tensor to 8 km depth in the KTB scientific drill holes: Implications for crustal strength, *J. Geophys. Res.*, *102*, 18,453-18,475, 1997.

Burkhard, M., Calcite twins, their geometry, appearance and significance as stress-strain markers and indicators of tectonic regime: A review, *J. Struct. Geol.*, *15*, 351-368, 1993.

Byerlee, J.D., Friction of rocks, *Pure Appl. Geophys.*, *116*, 615-626, 1978.

Craddock, J.P., and B.A. Van der Pluijm, Late Paleozoic deformation in the cratonic carbonate cover of eastern North America, *Geology*, *17*, 416-419, 1989.

Craddock, J.P., M. Jackson, B. Van Der Pluijm, and R.T. Versical, Regional shortening fabrics in eastern North America: Far-field stress transmission from the Appalachian-Ouachita orogenic belt, *Tectonics*, *12*, 257-264, 1993.

Craddock, J.P., J.N. Kimberly, and D.H. Malone, Calcite twinning strain constraints on the emplacement rate and kinematic pattern of the upper plate of the Heart Mountain Detachment, *J. Struct. Geol.*, *22*, 983-991, 2000.

Davis, D.M., and T. Engelder, Role of salt in fold-and-thrust belts, *Tectonophysics*, *119*, 67-88, 1985.

De Bresser, J.H.P., and C.J. Spiers, Strength characteristics of the r, f and c slip systems in calcite, *Tectonophysics*, *272*, 1-23, 1997.

Elliott, D., The energy balance and deformation mechanisms of thrust sheets, *Philos.Trans. R. Soc. London*, *283*, *Ser.A*, 289-312, 1976.

Engelder, T., A natural example of the simultaneous operation of free-face dissolution and pressure-solution, *Geochim. Cosmochim. Acta*, *46*, 69-74, 1982.

Engelder, T., and P. Geiser, Near-surface in situ stress, 4, Residual stress in the Tully Limestone Appalachian Plateau, New York, *J. Geophys. Res.*, *89*, 9365-9370, 1984.

Etchecopar, A., Etude des états de contraintes en tectonique cassante et simulation de déformations plastiques (approche mathématique), Ph.D. thesis, Univ. Montpellier, France, 1984.

Etchecopar, A., G. Vasseur, and M. Daignieres, An inverse problem in microtectonics for the determination of stress tensor from fault striation analysis, *J. Struct. Geol.*, *3*, 51-65, 1981.

Ferrill, D.A., Critical re-evaluation of differential stress estimates from calcite twins in coarse-grained limestones, *Tectonophysics*, *285*, 77-86, 1998.

Ferrill, D.A., and R.H. Groshong, Deformation conditions in the northern Subalpine Chain, France, estimated from deformation modes in coarse-grained limestones, *J. Struct. Geol.*, *15*, 995-1006, 1993a.

Ferrill, D.A., and R.H. Groshong, Kinematic model for the curvature of the northern Subalpine Chain, France, *J. Struct. Geol.*, *15*, 523-541, 1993b.

Gong, S.-Y., T.-Y. Lee, J.-C. Wu, S.-W. Wang, and K.-M. Yang, Possible links between the development of Plio-Pleistocene coral reef limestones and thrust migration in southwestern Taiwan, *J. Geol. Soc. China*, *39*, 151-166, 1996.

Gonzales-Casado, J.M., and C. Garcia-Cuevas, Calcite twins from microveins as indicators of deformation history, *J. Struct. Geol.*, *21*, 875-889, 1999.

Goodman, R., *Introduction to Rock Mechanics*, pp. 101-104, John Wiley, New York, 1989.

Groshong, R.H., Strain calculated from twinning in calcite, *Geol. Soc. Am. Bull.*, *83*, 2025-2048, 1972.

Groshong, R.H., Experimental test of least-squares strain gage calculation using twinned calcite, *Geol. Soc. Am. Bull.*, *85*, 1855-1864, 1974.

Groshong, R.H., O.A. Pfiffner, and L.R. Pringle, Strain partitioning in the Helvetic thrust belt of Eastern Switzerland from the leading edge of the internal zone, *J. Struct. Geol*, *6*, 5-18, 1984.

Harris, J.H., and B.A. Van der Pluijm, Relative timing of calcite twinning strain and fold-thrust belt development: Hudson Valley fold-thrust belt, New York, USA, *J. Struct. Geol.*, *20*, 21-31, 1998.

Ho, C.-S., A synthesis of the geologic evolution of Taiwan, *Tectonophysics*, *125*, 1-16, 1986.

Holl, J.E., and D.J. Anastasio, Cleavage development within a foreland fold and thrust belt, southern Pyrenees, Spain, *J. Struct. Geol.*, *17*, 357-369, 1995.

Hung, J.-H., Analysis of deformation fabrics in the Sani thrust sheet and the Chuhuangkeng anticline of western Taiwan, *Petrol. Geol. Taiwan*, *29*, 105-126, 1994.

Hung, J.-H., and C.-K. Kuo, Calcite twins for determining paleostrain and paleostress in the thrust front of the Taiwan collisional belt, *J. Geol. Soc. China*, *42*, 209-232, 1999.

Jackson, M., J.P. Craddock, M. Ballard, R. Van der Voo, and C. McCabe, Anhysteretic remanent magnetic anisotropy and calcite strains in Devonian carbonates from the Appalachian Plateau, New York, *Tectonophysics*, *161*, 43-53, 1989.

Jamison, W.R. and J. Spang, Use of calcite twin lamellae to infer differential stresses, *Geol. Soc. Am. Bull.*, *87*, 868-887, 1976.

Kohlstedt, D.L., and M.S. Weathers, Deformation-induced microstructures, paleopiezometers and differential stress in deeply eroded fault zones, *J. Geophys. Res.*, *85*, 6269-6285, 1980.

Lacombe, O., and P. Laurent, Determination of principal stress magnitudes using calcite twins and rock mechanics data, *Tectonophysics*, *202*, 83-93, 1992.

Lacombe, O., and P. Laurent, Determination of deviatoric stress tensors based on inversion of calcite twin data from experimentally deformed monophase samples: Preliminary results, *Tectonophysics*, *255*, 189-202, 1996.

Lacombe, O., J. Angelier, P. Laurent, F. Bergerat, and C. Tourneret, Joint analyses of calcite twins and fault slips as a key for deciphering polyphase tectonics : Burgundy as a case study, *Tectonophysics*, *182*, 279-300, 1990.

Lacombe, O., J. Bergues, J. Angelier, and P. Laurent, Quantification des paléocontraintes à l'aide des macles de la calcite: L'exemple de la compression pyrénéo-provençale au front de la Montagne Sainte-Victoire (Provence), *C. R. Acad. Sci., Ser.II*, 313, 1187-1194, 1991.

Lacombe, O., J. Angelier, and P. Laurent, Les macles de la calcite, marqueurs des compressions récentes dans un orogène actif: L'exemple des calcaires récifaux du sud de Taiwan, *C.R. Acad. Sci., Ser.II*, 306, 1805-1813, 1993.

Lacombe, O., P. Laurent, and J. Angelier, Calcite twins as a key to paleostresses in sedimentary basins: Preliminary results from drill cores of the Paris basin, in *Peri-Tethyan Platforms*, edited by F. Roure, pp. 197-210, Editions Technip, Paris, 1994.

Lacombe, O., J. Angelier, M. Rocher, J. Bergues, H.-T. Chu, B. Deffontaines, and J.-C. Hu, Contraintes et plissement au front d'une chaîne de collision: L'exemple des calcaires récifaux pliocènes de Yutengping (Taiwan), *Bull. Soc. Géol. Fr.*, *167*, 361-374, 1996.

Lacombe, O., F. Mouthereau, B. Deffontaines, J. Angelier, H.-T. Chu, and C.-T. Lee, Geometry and Quaternary kinematics of fold-and-thrust units of southwestern Taiwan, *Tectonics*, *18*, 1198-1223, 1999.

Laurent, P., Les macles de la calcite en tectonique: Nouvelles méthodes dynamiques et premières applications, Ph.D. thesis, Univ. Montpellier, France, 1984.

Laurent, P., H. Kern, and O. Lacombe, Determination of deviatoric stress tensors based on inversion of calcite twin data from experimentally deformed monophase samples, part II, Uniaxial and triaxial stress experiments, *Tectonophysics*, *327*, 131-148, 2000.

Laurent, P., P. Bernard, G. Vasseur, and A. Etchecopar, Stress tensor determination from the study of e twins in calcite: A linear programming method, *Tectonophysics*, *78*, 651-660, 1981.

Laurent, P., C. Tourneret, and O. Laborde, Determining deviatoric stress tensors from calcite twins: Application to monophased synthetic and natural polycrystals, *Tectonics*, *9*, 379-389, 1990.

Lespinasse, M., and M. Cathelineau, Paleostress magnitudes determination by using fault slip and fluid inclusions planes data, *J. Geophys. Res.*, *100*, 3895-3904, 1995.

Lin, C.-W., and Y.-B. Lee, Calcite twin analysis of the Tungho and Kangkou limestones in the Coastal Range, eastern Taiwan, *J. Geol. Soc. China*, *40*, 639-652, 1997.

Mouthereau, F., B. Deffontaines, O. Lacombe, and J. Angelier, Along-strike variations of the Taiwan belt front: Basement control on structural style, wedge geometry and kinematics, *Geol. Soc. Am. Spec. Pap.*, *358*, in press, 2001a.

Mouthereau, F., O. Lacombe, B. Deffontaines, J. Angelier, and S. Brusset, Deformation history of the southwestern Taiwan foreland thrust belt: Insights from tectono-sedimentary analysis and balanced cross-sections, *Tectonophysics*, *333*, 293-322, 2001b.

Newman, J., The influence of grain size and grain size distribution on methods for estimating paleostresses from twinning in carbonates, *J. Struct. Geol.*, *16*, 1589-1601, 1994.

Onasch, C.M., Dynamic analysis of rough cleavage in the Martisburg Formation, Maryland, *J. Struct. Geol.*, *5*, 73-82, 1983.

Petit, J.P., La zone de décrochements du Tizi N'Test (Maroc) et son fonctionnement depuis le Carbonifère, Ph.D. thesis, Univ. Montpellier, France, 1976.

Pfiffner, O.A., Deformation mechanisms and flow regimes in limestones from the Helvetic zone of the Swiss Alps, *J. Struct. Geol.*, *4*, 429-442, 1982.

Rocher, M., Déformations et paléocontraintes des avant-pays de chaînes de collision: Les piémonts occidentaux de Taiwan et le bassin sud-aquitain, Ph.D. thesis, Univ. P. et M. Curie, Paris, France, 1999.

Rocher, M., O. Lacombe, J. Angelier, and H.-W. Chen, Mechanical twin sets in calcite as markers of recent collisional events in a fold-and-thrust belt: Evidence from the reefal limestones of southwestern Taiwan. *Tectonics*, *15*, 984-996, 1996.

Rocher, M., O. Lacombe, J. Angelier, B. Deffontaines, and F. Verdier, Cenozoic folding and faulting in

the North Pyrenean Foreland (Aquitaine Basin, France): Insights from combined structural and paleostress analyses, *J. Struct. Geol.*, *22*, 627-645, 2000.

Rowe, K.J., and E.H. Rutter, 1990. Paleostress estimation using calcite twinning: Experimental calibration and application to nature, *J. Struct. Geol*, *12*, 1-17, 1990.

Spiers, C.J., The development of deformation textures in calcite rocks, Ph.D. thesis, Univ. of London, England, UK, 1982.

Spiers, C.J., and H.R. Wenk, Evidence for slip on r and f in the positive sense in deformed calcite single crystals, *EOS Trans. AGU*, *61*, 1128, 1980.

Teufel, L.W., Strain analysis of experimental superposed deformation using calcite twin lamellae, *Tectonophysics*, *65*, 291-309, 1980.

Tourneret, C., and P. Laurent, Paleostress orientations from calcite twins in the north pyrenean foreland determined by the Etchecopar inverse method, *Tectonophysics*, *180*, 287-302, 1990.

Tschanz, X., Analyse de la déformation du Jura central entre Neuchatel (Suisse) et Besançon (France), *Eclogae geol. Helv.*, *88*, 543-558, 1990.

Tullis, T.E., The use of mechanical twinning in minerals as a measure of shear stress magnitudes, *J. Geophys. Res.*, *85*, 6263-6268, 1980.

Turner, F.J., Nature and dynamic interpretation of deformation lamellae in calcite of three marbles, *Am. J. Sci.*, *251*, 276-298, 1953.

Turner, F.J., and H.C. Heard, Deformation in calcite crystals at different strain rates, *Univ. Calif. Publ. Geol. Sci.*, *46*,103-126, 1965.

Turner, F.J., D.T. Griggs, and H.C. Heard, Experimental deformation of calcite crystals, *Geol. Soc. Am. Bull.*, *65*, 883-934, 1954.

Twiss, R.J., Theory and applicability of a recrystallized grain size paleopiezometer, *Pure Appl. Geophys.*, *115*, 227-234, 1977.

Van der Pluijm, B.A., J.P. Craddock, B.R. Graham, and J.H. Harris, Paleostress in cratonic north America: Implications for deformation of continental interiors, *Science*, *277*, 794-796, 1997.

Weathers, M.S., J.M. Bird, R.F. Cooper, and D.L. Kohlstedt, Differential stress determined from deformation-induced microstructures of the Moine thrust zone, *J. Geophys. Res.*, *84*, 7495-7509, 1979.

Wenk, H.R., H. Kern, P. VanHoutte, and F. Wagner, Heterogeneous strain in axial deformation of limestone, textural evidence, in Mineral and Rock Formation: Laboratory studies, Geophys. Monogr., vol. 36, edited by B.E. Hobbs and H.C. Heard, pp 287-295, AGU, Washington, D.C., 1986.

Zoback, M.D., R. Apel, J. Baumgärtner, M. Brudy, R. Emmermann, B. Engeser, K. Fuchs., W. Kessels, H. Rischmüller, F. Rummel, and L. Vernik, Upper-crustal strength inferred from stress measurements to 6km depth in the KTB borehole, *Nature*, *365*, 633-634, 1993.

O. Lacombe, Laboratoire de Tectonique, Université Pierre et Marie Curie, T26-25, E1, Boîte 129, 4 pl. Jussieu, F-75252 Paris Cedex 05, France. (olivier.lacombe@lgs.jussieu.fr)

(Received January 3, 2001;
revised June 20, 2001;
accepted June 26, 2001.)